Glass Transition Temperatures of Hydrocarbon Blends: Adhesives Measured by Differential Scanning Calorimetry and Dynamic Mechanical Analysis

ADAM S. CANTOR*

3M Masking and Packaging Systems Division, 3M Center, Building 230-1S-14, St. Paul, Minnesota 55144-1000

ABSTRACT: A comparison of calculated and measured glass transition temperatures of a series of three-component hydrocarbon blends was performed. The blends were prepared as mixtures of an elastomer with different proportions of tackifying resin and oil. Glass transition temperature, T_g, was measured by differential scanning calorimetry (DSC) and dynamic mechanical analysis (DMA) at four measurement frequencies. Most of these blends had pressure-sensitive adhesive (PSA) properties, and were used to prepare a series of PSA tapes. The adhesion of the PSA tapes was shown to be strongly dependent on T_g. Tack of PSA tapes was measured at two different temperatures, and shown to be directly correlated to the blend T_g. Several predictive methods for blend T_g that are based on individual component T_gs were evaluated. The prediction of blend T_g is far more accurate if the individual component T_g values are determined by DMA instead of DSC. In addition, the Gordon-Taylor equation gave a significant improvement on predicted blend T_g when compared to the Fox equation. © 2000 John Wiley & Sons, Inc. J Appl Polym Sci 77: 826–832, 2000

Key words: glass transition temperature; blends; pressure-sensitive adhesive; dynamic mechanical analysis; differential scanning calorimetry

INTRODUCTION

Pressure-sensitive adhesive (PSA) properties are known to depend strongly on the glass transition temperature of the adhesive.[1] Exploiting this correlation can be complex, however, because there is more than one way to measure glass transition temperature, T_g, and the value of T_g can strongly depend on the measurement method. Many adhesives are either copolymers, blends of polymers, blends of polymer with low molecular weight diluents, or some combination of these. Therefore, there is a strong desire to be able to calculate a T_g for a mixture based on the T_gs of the individual components in the mixture. This allows for predictions of adhesive properties prior to synthesizing materials, ease in experimental design when working with mixtures, alleviates the need to do many time-consuming measurements of T_g, and aids in understanding experimental results.

In general, when studying blends, the presence of a single T_g is used as evidence of a miscible blend. A number of theories[2–10] have been put forth for predicting the T_g of copolymers or miscible polymer blends based on the individual component T_gs of the blend, and these may also be applied to blends of polymers with lower molecular weight diluents. Due to the weak entropic contribution to the free energy of polymer blends, the formation of miscible polymer blends often depends on specific enthalpic interactions[10] that

Table I

Component	MW (g/mol)	Density (g/cm^3)	Comments
Kraton D1107-P	200,000[a]	0.90[d,e]	S-I-S, 14% styrene, 15% S-I diblock
Escorez 1310LC	M_n = 700	0.97[e]	C-5 aliphatic hydrocarbon
	M_w = 1400[b]		
Shellflex 371N	410[c]	0.88[e]	Naphthenic/paraffinic oil

[a] S-I-S peak molecular weight. Polystyrene equivalent MW measured by gel permeation chromatography.

[b] Polystyrene equivalent MWs measured by gel permeation chromatography.

[c] Ebullioscopic methods of Mechrolah osmometer (ref. 15).

[d] The density of the isoprene phase was estimated by extrapolating the densities of similar SIS rubbers containing 22 and 30% styrene, with densities of 0.93 and 0.94, respectively. Thus a density of 0.90 g/cm^3 was taken for the isoprene phase of the Kraton rubber.

[e] Values are taken from standard product literature.

can have significant effects on the blend T_g. For this reason, a number of theoretical treatments have met with variable predictive success, depending on the particular blend systems studied.[3–14]

In this study, rubber–resin–oil mixtures of a type used in packaging tape pressure-sensitive adhesives (PSAs) were prepared and measured by both Differential Scanning Calorimetry (DSC) and Dynamic Mechanical Analysis (DMA). Because of the relatively low molecular weight of the resin and oil, these blends are miscible, despite the lack of any particular enthalpic contribution to the free energy of mixing. The results obtained from these studies were compared both to PSA tape properties and to several theoretical predictions for blend glass transition temperatures.

EXPERIMENTAL

The pressure-sensitive adhesives were prepared from three components (see Table I for individual component details). The rubber was Kraton D1107-P (Shell Chemical Co.), an S-I-S elastomer. The tackifier was Escorez 1310LC (Exxon Chemical Co.), a low molecular weight C5 hydrocarbon resin. The plasticizer was Shellflex 371N (Shell Chemical Co.), a naphthenic/paraffinic oil. All materials were used as received.

Mixtures were prepared as solutions in toluene. No antioxidants were used. Adhesive tapes were prepared by knife coating to a nominal dry coating weight of 27 g/m^2 onto 50 micron-thick biaxially oriented polypropylene. Samples were dried at 65°C for 15 min.

The amount of rubber in all of the formulations was 44.6%. The amount of solid tackifier varied from 55.4 to 0%, with the remainder of the formulation consisting of oil.

Dynamic mechanical analysis (DMA) was done on a Rheometrics RDA2 torsion rheometer using a liquid nitrogen cooling unit. Adhesive samples for rheometry were prepared by solvent casting disks of 1.0 to 1.5-mm dry thickness. A single solvated layer was cast, and the solvent was allowed to very slowly evaporate over several days to ensure homogenous and bubble-free samples. After this slow air drying the samples were further dried under vacuum for at least 8 h.

DMA data was collected at 1, 10, 100, and 500 rad/s frequencies during temperature scans covering the glass transition region for each sample. Temperature steps of 5°C with 90-s soak times were used. Use of 8-mm sample plates was necessary to obtain the width of the glass transition. Measurements with 25-mm sample plates gave complete agreement with the T_g values obtained with the 8-mm plates.

The pure Kraton D1107 rubber sample was prepared and measured in the same fashion as the adhesive samples for DMA.

DMA measurements of the Escorez 1310LC were done with the resin suspended in silicone rubber. The silicone rubber has a very moderate change in tan δ, so the glass transition due to the resin appears as a peak on a sloping baseline. The resin was also measured as a neat sample. This required heating the resin with a heat gun just until it softened into a malleable material. This softened mass was then compressed between preheated rheometer plates. The T_gs obtained with this method were equivalent to those using the silicone suspension. Care has to be taken during this measurement, however, as the resin is undergoing extreme

Table II

Method	Frequency (DMA, rad/s)	Rubber T_g (K)	Resin T_g (K)	Oil T_g (K)
DSC	—	215	314	209
DMA	1	217	355	215
DMA	10	221	358	220
DMA	100	226	365	226
DMA	500	230	372	233

changes in modulus with temperature. Thus, stress levels and sample integrity need to be closely monitored to avoid spurious results. Although more difficult in practice, this does have the advantage of a stronger signal, as well as providing quantitative measurements of tan δ and storage modulus for the resin.

The oil was absorbed into a polyethylene sponge. The sponge was connected to parallel plates using a transfer tape adhesive. The dry sponge/transfer tape composite showed little change in tan δ over the temperature range of −70 to 0°C. As in the case with the resin in silicone suspension, the glass transition of the oil appears as a peak on a sloping baseline.

Differential scanning calorimetry (DSC) measurements were done on a TA DSC 2920 with a TA 2200 data system. Scans were run at 10°C/min heating rates, using approximately 10-mg samples in crimped aluminum pans. The T_gs were calculated both at half height and at the inflection point.

Adhesion testing was done following ASTM D3330-90, "Peel Adhesion of Pressure-Sensitive Tape at 180° angle." Tack measurements were done with a variation of ASTM D3121-94, "Tack of Pressure-Sensitive Adhesives by Rolling Ball." Instead of a ball, however, a wheel was allowed to roll down an inclined plane and across an up-turned adhesive surface. This method is similar to the rolling ball standard, in that the tack is reported in millimeters of travel, with lower numbers representing better tack. Values of 300 mm represent an upper limit for this test.

Adhesion and tack tests were performed in a controlled temperature and humidity testing room (23°C/50%RH). Tack tests were also performed in a controlled temperature testing room at 4°C. Tape property tests were the average of two individual measurements.

RESULTS AND DISCUSSION

Initially, glass transition temperatures were calculated using the Fox equation:[2]

$$\frac{1}{CT_g} = \frac{x_1}{T_{g1}} + \frac{x_2}{T_{g2}} + \frac{x_3}{T_{g3}} \tag{1}$$

where CT_g is the calculated glass transition temperature, x_1, x_2, and x_3 are the weight fractions of the adhesive components, and T_{g1}, T_{g2}, and T_{g3} are the T_gs for the individual components. The weight of the rubber fraction is taken as the amount of isoprene in the Kraton rubber. The DMA measured T_gs at four different frequencies and the DSC T_gs for the individual components are shown in Table II. As they are generally more readily available, the DSC T_gs were used for purposes of calculation unless otherwise noted.

Tape Properties Versus Calculated $T_{g\text{-DSC}}$

As expected, the tape properties showed a strong dependence on the glass transition temperature. The adhesion to steel showed a steady decrease with decreasing CT_g shown in Figure 1. The adhesion was highest for the mixture with no oil, and decreased nearly linearly until the CT_g was approximately 235 K. All of the mixtures below 230 K had very low adhesion.

Tack showed an even stronger dependence on CT_g at both room temperature (23°C) and cold temperature (4°C) shown in Figure 2. At room temperature the tack was poor (i.e., maximum value) for $CT_g \geq -8°C$ (265 K) and good for CT_gs

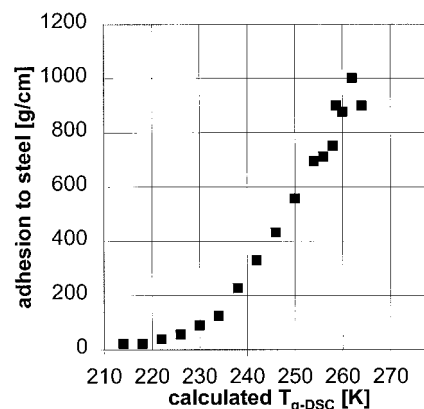**Figure 1** Adhesion to steel as a function of calculated $T_{g\text{-DSC}}$ (using DSC component values and the Fox equation).
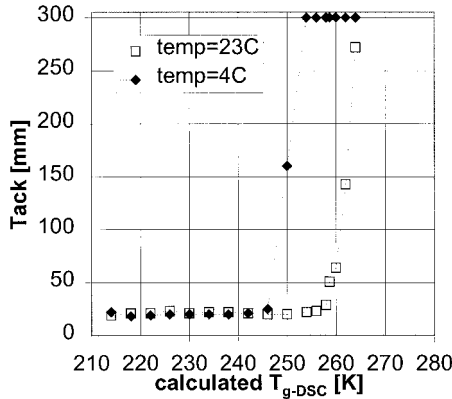
Figure 2 Tack as a function of calculated $T_{g\text{-DSC}}$ (using DSC component values and the Fox equation).

Figure 4 T_g measured with both DMA and DSC as a function of calculated $T_{g\text{-DSC}}$ (using DSC component values and the Fox equation).

$\leq -18°C$ (255 K). A response between 20 and 300 mm was only seen over a 10°C range of CT_g. At cold temperature this response range was between -20 and $-30°C$. It is interesting to note that although the testing temperature was lowered by 19°C, the change in CT_g between the two response ranges was only 12°C.

This data was also compared to T_g data measured using DMA. When plotted against the actual $T_{g\text{-DMA}}$ of the samples, the shift in response between room and cold temperature data sets was 17°C. This was observed for all four frequencies, and is shown in Figure 3 for 100 rad/s data. This agrees quite well with the expected 19°C shift that would be observed if the tack were solely dependent on the T_g of the formulation.

In addition to T_g, the plateau storage modulus for an adhesive can also have a significant effect on tape properties. In simple terms, this is described by the Dahlquist criterion indicating the
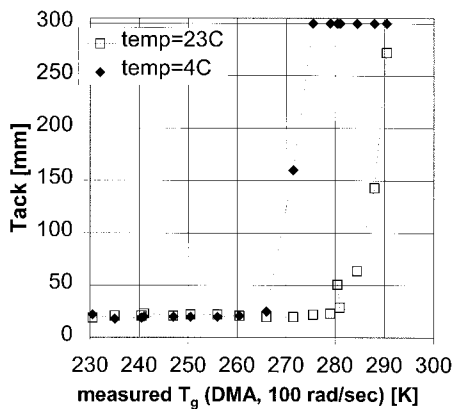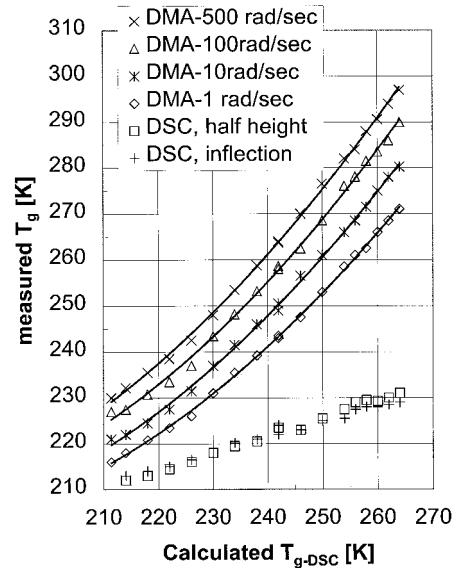
maximum allowable storage modulus for a pressure-sensitive adhesive.[1] The simplest description of tackified rubbers predicts that the plateau modulus should depend on the rubber fraction and the type of the rubber.[14] Thus, the samples here would be predicted to all have the same plateau modulus. Actually, the plateau storage modulus (ω at 1 rad/s), G'_{plateau}, decreased from approx. 7×10^5 dyne/cm^2 to approximately 5×10^5 dyne/cm^2 with decreasing T_g. Decreases of a similar magnitude are seen at the other frequencies measured. This shift is relatively minimal compared to the change in glass transition temperature, however, so it is not expected that changes in adhesive properties were significantly affected by changes in G'_{plateau}.

Measured T_g Versus Calculated $T_{g\text{-DSC}}$

A comparison of the measured T_g values was made to the calculated T_g values (using DSC input values and the Fox equation). This is shown in Figure 4. The $T_{g\text{-DMA}}$ is offset from the CT_g, depending on the frequency. The change in $T_{g\text{-DMA}}$ over the entire range of CT_g studied was nearly linear, but there was some curvature in the dependence. A quadratic polynomial fit to the data is shown for each frequency, and this fit is superior to a linear fit with 95+% confidence. At high T_g the $T_{g\text{-DMA}}$ changes faster than the CT_g

Figure 3 Tack as a function of T_g at 100 rad/s (measured by DMA).

(slope ~1.3 to 1.4), whereas at very low T_g it changes slower than the CT_g (slope ~0.6 to 1.0).

The $T_{g\text{-DSC}}$ agrees with the CT_g for the low T_g sample, but does not agree with the increase predicted by the CT_g for the higher T_g samples. The $T_{g\text{-DSC}}$ changes much less than predicted by the CT_g (slope ~0.4), making DSC only weakly sensitive to changes in formulation. As shown previously, adhesives with CT_gs that differ by 10°C can have dramatically different properties, yet they can show nearly identical $T_{g\text{-DSC}}$. This weak sensitivity of $T_{g\text{-DSC}}$ to changes in CT_g reduces the value of using DSC to measure T_g of these blends.

Measured T_g Versus Calculated $T_{g\text{-DMA}}$

Because of the large disagreement between calculated and measured T_gs using DSC, a comparison was made of calculated and measured T_gs using DMA. The $CT_{g\text{-DMA}}$ values were also calculated using the Fox equation, but with the appropriate DMA input value for the frequency of interest (see Table II). A comparison of DMA measured T_gs for four different frequencies are shown in Figure 5 as a function of $CT_{g\text{-DMA}}$.

The variation with frequency of the adhesive T_g is now compensated by the variation with frequency of the component T_gs. The agreement at the lowest T_gs is not surprising, because the oil and rubber have similar T_gs. Thus, a blend of rubber and oil would be expected to have a T_g similar to either component. The agreement at higher T_gs, however, indicates substantial success of the Fox prediction. The agreement is best for high-frequency DMA (500 rad/s), but is still fairly good at low frequency (1 rad/s) also.
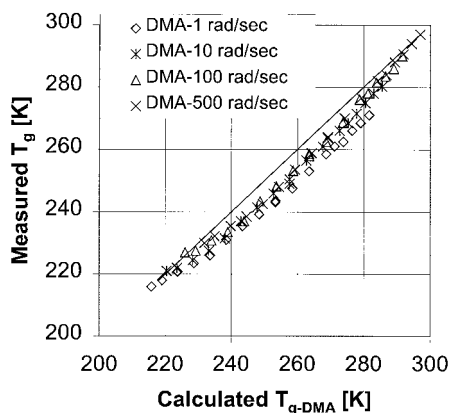

Figure 5 T_g measured with DMA as a function of calculated $T_{g\text{-DMA}}$ (using DMA component values and the Fox equation).
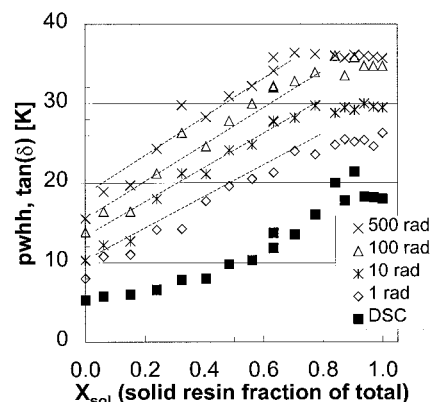

Figure 6 Width of the blend glass transition as a function of solid resin fraction.

One other interesting observation was the width of the glass transition. The transition was broadest when the tackifier was 100% solid resin. As the oil percentage increased, the transition narrowed. This could be indicative of better solubility of the oil in the rubber. This was true for both DMA and DSC measurements, and is shown in Figure 6.

A further curiosity of this transition width was the lack of change in transition width at high solid resin fraction. When the solid resin fraction exceeds 0.6 to 0.8 of the total tackifier then the glass transition width ceases to increase. Although not well understood, this may indicate that these concentrations are near to or above the maximum solubility of the resin in the isoprene phase of the rubber.

Calculating Glass Transition Temperature–Theory

The previous results in this article are compared to the glass transition temperature calculated using the Fox equation. A number of other methods[3–8] were also be used to calculate the blend T_g.

$$T_g = x_1 T_{g1} + x_2 T_{g2} + x_3 T_{g3} \tag{2}$$

$$\ln(T_g) = x_1\ln(T_{g1}) + x_2\ln(T_{g2}) + x_3\ln(T_{g3}) \tag{3}$$

$$T_g = \frac{x_1 T_{g1} + K x_2 T_{g2} + K' x_3 T_{g3}}{x_1 + K x_2 + K' x_3} \tag{4}$$

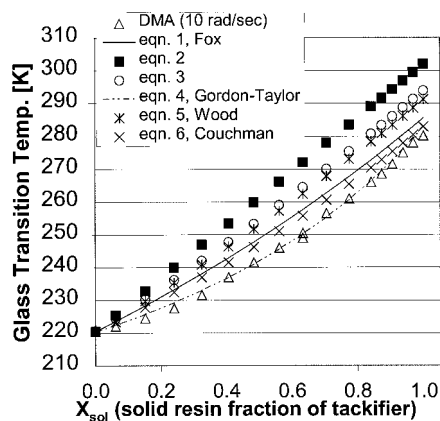where

$$K = \frac{\rho_1 T_{g1}}{\rho_2 T_{g2}}$$

Figure 7 Several theoretical predictions for calculated $T_{g\text{-DMA}}$ (using DMA component values) compared to T_g measured with DMA at 10 rad/s.

and

$$K' = \frac{\rho_1 T_{g1}}{\rho_3 T_{g3}}$$

and ρ_1, ρ_2, and ρ_3 are the component densities.

$$T_g = \frac{x_1 \Delta C_{p1} T_{g1} + x_2 \Delta C_{p2} T_{g2}}{x_1 \Delta C_{p1} + x_2 \Delta C_{p2}} \quad (5)$$

$$\ln(T_g) = \frac{x_1 \Delta C_{p1} \ln(T_{g1}) + x_2 \Delta C_{p2} \ln(T_{g2})}{x_1 \Delta C_{p1} + x_2 \Delta C_{p2}} \quad (6)$$

In all cases, x_1, x_2, and x_3 are the weight fractions of the adhesive components, and T_{g1}, T_{g2}, and T_{g3} are the T_gs for the individual components. C_p is the change in heat capacity between the liquid and glassy state.

Comparisons to measured DMA T_gs taken at a frequency of 10 rad/s are shown in Figure 7 for the different theories. Individual component T_gs were taken from DMA T_gs measured at 10 rad/s.

Equations (2) and (3) are additive approaches that are calculationally very convenient, but they provide poorer agreement with the experimental data than the Fox equation.

Equation 4 is the Gordon-Taylor equation.[5] This is essentially identical to the Fox equation, except the weight fractions are replaced by volume fractions. The form of the equation looks different, because it is still expressed in weight fractions. This provides a significantly better fit to the experimental data. The primary reason for this is that the solid resin is more dense than the other components and has a higher T_g than the

other components. Therefore, in this case the Gordon-Taylor equation predicts a lower blend T_g than the Fox equation prediction, and gives better agreement with the experimental measurement.

Equations (5) and (6) (Wood[3] and Couchman[4] equations) take into account the differing heat capacities of each component. Neither equation provided a significant improvement over the Fox equation.

The only significant improvement on the Fox equation is found using the Gordon-Taylor equation. This gives a much better fit to the experimental data, with an average deviation between calculated and experimental values of 1.0°C. Although somewhat more complicated, because component densities are needed as input data, this does provide a significant improvement over the Fox equation without the addition of any adjustable parameters.

CONCLUSION

The glass transition temperature of an adhesive is an important indicator of physical tape properties. It is also well known that the adhesive T_g can be calculated from the amounts and T_gs of the individual components in a mixture. It has been common practice to use individual component values of T_g determined using DSC. Although the general trends of the predicted T_gs correspond to the actual T_g, there is not a good quantitative correlation when using DSC.

It is shown here that using individual component values of T_g determined using DMA gives a very strong correlation between predicted and actual T_gs measured by DMA. The Fox equation provides a fairly good prediction of the observed DMA T_gs. Use of the Gordon-Taylor equation provides an even more accurate prediction of DMA T_gs with an average deviation between measured and predicted T_gs of only 1.0°C over a range of blend T_gs spanning 65°C.

Use of DMA calculated T_gs can provide for improved formulating in designed experiments, as well as improved understanding of the relationship between adhesive material properties and measured tape properties.

Rooke for performing the adhesion testing, and David Yarusso for helpful discussions.

REFERENCES

1. Chu, S. G. In Handbook of Pressure Sensitive Adhesive Technology; Satas, D., Ed.; Van Nostrand Reinhold: New York, 1989.
2. Fox, T. G. Bull Am Phys Soc 1956, 1, 123.
3. Wood, L. A. J Polym Sci 1958, 28, 319.
4. Couchman, P. R. Macromolecules 1978, 11, 1156.
5. Gordon, J. S.; Taylor, J. S. J Appl Chem 1952, 2, 493.
6. Brekner, M.-J.; Schneider, H. A.; Cantow, J.-J. Polymer 1988, 29, 78.
7. Couchman, P. R. Macromolecules 1987, 20, 1712.
8. Couchman, P. R. Macromolecules 1991, 24, 5772.
9. Boyer, R. F. J Macromol Sci Phys 1973, B7, 487.
10. Lu, X.; Weiss, R. A. Macromolecules 1992, 25, 3242.
11. Krause, S.; Roman, N. J Polym Sci Part A 1965, 3, 1631.
12. Schneider, H. A.; Leikauf, B. Thermochim Acta 1987, 114, 165.
13. ten Brinke, G.; Karasz, F. E.; Ellis, T. S. Macromolecules 1983, 16, 244.
14. Kraus, G.; Rollmann, K. W. J Appl Polym Sci 1977, 21, 3311.
15. Ewins, E. E., Jr.; St. Clair, D. J.; Erickson, J. R.; Korcz, W. H. In Handbook of Pressure Sensitive Adhesive Technology; Satas, D. Ed.; Van Nostrand Reinhold: New York, 1989.